# Evidence for a Cosmological Constant and for the Expansion of the Universe*

GERSON GOLDHABER† for the Supernova Cosmology Project‡
Institute for Nuclear and Particle Astrophysics
Lawrence Berkeley National Laboratory
& Center for Particle Astrophysics
University of California at Berkeley
Berkeley, California 94720, USA

*This work was supported in part by the United States Department of Energy, contract numbers DE-AC03-76SF00098, CfPA, and NSF contract number AST-9120005

†Talk presented at the XXVI SLAC Summer Institute on Particle Physics 1998, GRAVITY from the Hubble Length to the Planck Length, gerson@lbl.gov

‡G. Aldering[a], B.J. Boyle[b], P.G. Castro[a], W.J. Couch[c], S. Deustua[a], S. Fabbro[d], R.S. Ellis[e], A.V. Filippenko[f], A. Fruchter[g], G. Goldhaber[a], A. Goobar[h], D.E. Groom[a], I.M. Hook[i], M. Irwin[e], A.G. Kim[j], M.Y. Kim[a], R.A. Knop[a], J.C. Lee[e], T. Matheson[f], R.G. McMahon[e], H.J.M. Newberg[n], C. Lidman[o], P. Nugent[a], N.J. Nunes[a], R. Pain[d], N. Panagia[g], C.R. Pennypacker[a], S. Perlmutter[a], R. Quimby[a], P. Ruiz-Lapuente[k], B. Schaefer[l] and N. Walton[m]. (*a*) LBNL Berkeley California, (*b*) Anglo-Australian Observatory, Sydney, (*c*) University of New South Wales, Sidney, (*d*) LPNHE, CNRS-IN2P3, University of Paris VI & VII, (*e*) Institute of Astronomy, Cambridge U.K., (*f*) Dept. of Astronomy, Univ. of California, Berkeley, (*g*) Space Telescope Science Inst., Baltimore, Maryland, (*h*) Dept of Physics, Stockholm Univ., Sweden, (*i*) Inst. of Astronomy, Univ. of Edinburgh U.K. , (*j*) L.P.C.C. College de France, Paris, (*k*) Dept. of Astronomy, Univ. of Barcelona, Spain, (*l*) Dept.of Astronomy, Yale Univ., New Haven Connecticut, (*m*) Isaac Newton Group, La Palma, Spain, (*n*) FNAL Batavia, Illinois, (*o*) ESO, La Scilla, Chile

ABSTRACT

A search for cosmological supernovae has discovered over 75, most of which are type Ia supernovae (SNe Ia). There is strong evidence from measurements of nearby type Ia supernovae that they can be considered as distance indicators or "standard candles" after correction for the width (time scale stretch parameter) of the individual light curves. Measurements and analysis are completed on 42 of these distant, $z$=0.18 to 0.83, supernovae. These supernovae, together with 18 "nearby," $z < 0.11$ supernovae from the Calán/Tololo Supernova Survey allow us to measure the ratio of the matter density of the universe to the critical density $\Omega_M$ together with the normalized cosmological constant $\Omega_\Lambda$, the energy density of the vacuum. For a flat universe, i.e. $\Omega_M + \Omega_\Lambda = 1$, we obtain $\Omega_M = 0.28\ ^{+0.09}_{-0.08}$ (statistical) $^{+0.05}_{-0.04}$ (systematic). The data are strongly inconsistent with a $\Lambda = 0$ flat cosmology, the simplest inflationary universe model. An open, $\Lambda = 0$ cosmology also does not fit the data well: the data strongly suggest that the cosmological constant is non-zero and positive, with a confidence of $P(\Lambda > 0) > 99\%$. By treating 36 of our high z SNe Ia with $0.30 < z < 0.70$ as a group we find that the expected light curve widths based on the nearby width-distribution, is in agreement with the observed distribution. In particular we demonstrate that when normalized our SNe fit a single curve with a single parameter stretch, $s$. We also obtain a direct confirmation of the hypothesis that extra-galactic redshifts are due to cosmological expansion by observing the expected "time dilation" Doppler shift $1 + z$ of SNe Ia light curves at high redshift.

## 1. The Matter Density and Vacuum Energy Density of the Universe

When Einstein introduced his General Theory of Relativity (1916) the universe was assumed to be static. To accomplish such a static universe Einstein had to introduce a repulsive force corresponding to a "cosmological constant," $\Lambda$, to compensate for the gravitational attraction of the matter in the universe. Later, when Hubble discovered that the universe was actually expanding (1924), Einstein called the cosmological constant "his greatest mistake." All the same, since $\Lambda$ is consistent with Einstein's theory one need not assume that $\Lambda = 0$. Thus the value of $\Lambda$ becomes an experimental question. Here $\Omega_\Lambda$ the vacuum energy density, is given by $\Omega_\Lambda = \Lambda/(3H_0^2)$ and $\Omega_M$ is the matter density of the universe. In our current study we primarily obtain a linear combination of these two densities.

When we started out with this study, ten years ago, we were planning to measure the deceleration of the universe $q_0$. On the then prevalent assumption (prejudice) that $\Omega_\Lambda = 0$ we expected a positive deceleration of the universe due to the matter density. With our present observations we find, to a high probability $P(\Lambda > 0) > 99\%$, that $q_0$ is actually negative, corresponding to an acceleration of the expansion of the universe! Our best fit corresponds to the relation $0.8\Omega_{\rm M} - 0.6\Omega_\Lambda \approx -0.2 \pm 0.1$. For a flat, $\Omega_M + \Omega_\Lambda = 1$, cosmology this corresponds to $\Omega_M = 0.28\ ^{+0.09}_{-0.08}$ (statistical) $^{+0.05}_{-0.04}$ (systematic).

Before our present work started, estimates of $\Omega_M$, based on a variety of experiments, ranged from 0.05 to 1.5. Since the light emitting matter contributes roughly

0.01 to $\Omega_M$, a measurement of $\Omega_M$ also determines the contribution of dark matter to the universe.

## 2. Type Ia SNe as Calibrated Standard Candles?

There is good evidence that type Ia supernovae (SNe Ia), the brightest of all the different types of SNe, can be calibrated to have a standard brightness. A plausible explanation for this behavior is that SNe Ia are the consequence of the explosion of a white dwarf star as it approaches a critical mass, of 1.4 solar masses, the Chandrasekhar limit.

A white dwarf is a star that has burnt all of its hydrogen and helium by fusion primarily to carbon and oxygen and as a result has collapsed under the gravitational force to a degenerate electron gas in which the C and O nuclei are embedded. The white dwarf thus has the mass of the order of the mass of the sun but a radius comparable to that of the earth. If this white dwarf is in a binary system with another star, a common occurrence, the companion star can transfer matter to the white dwarf until it approaches the Chandrasekhar limit. Near this mass, the electron degeneracy pressure can no longer support the star and a runaway thermonuclear explosion occurs.

In this supernova explosion, the temperature and density reach the point at which the C and O nuclei fuse and produce higher mass nuclei. The fusion process stops at $^{56}$Ni, a radioactive isotope with equal number of protons and neutrons. In fact, an enormous amount of $^{56}$Ni is produced, typically 0.6 of a solar mass. In the expolsion the newly produced material is ejected with velocities of about 10,000 km/sec to 30,000 km/sec. At first, the exploding star is too small to be seen. Over a period of a few days, however, it expands rapidly and its brightness reaches a maximum value in about 18 days in the rest system. It is during this period that we first discover the SN as we will describe below. The light observed is produced by ionization from the decay products of $^{56}$Ni and its daughter isotope $^{56}$Co. The $^{56}$Ni isotope has a half life of about 6 days and $^{56}$Co has a half life of 77 days, so it is primarily the $^{56}$Co decay that is powering the supernova at maximum light. Finally $^{56}$Co decays to stable $^{56}$Fe.

All the same, not all SNe Ia have exactly the same brightness at the peak of the lightcurve. There is a dispersion of about 0.24 to 0.5 magnitudes (depending on the sample selection criteria) in the maximum brightness distribution.[15] Phillips[1] noted a correlation between the brightness and the decline rate of the SNe Ia. We express this correlation (Perlmutter et al., 1997)[2] in terms of a stretch parameter $s$ applied to the time axis in the lightcurve of the SN. Thus $s$ affects both the rise rate and the decline rate of the SN. The greater $s$, meaning the wider the SN light curve, with reference to the standard Leibundgut[3] curve, the brighter it is. We measure typical values for $s$ from 0.8 to 1.2 with a few outliers above and below these values. We find a correction to the B-band absolute magnitude $M$ of $-\alpha(s-1)$. In our analysis we apply this correction to the apparent magnitude $m_B$ giving an effective magnitude $m_B^{\rm effective} = m_B + \alpha(s-1)$ which then corresponds to a unique value of

the absolute magnitude $M$, with an uncertainty of approximately 0.17 magnitudes, or $\sim$17% in flux. (This dispersion can be improved still further with multiple filter-band constraints on extinction; see discussions in Perlmutter et al.[6] and references therein.) In theoretical models, it has been suggested that this lightcurve width-luminosity relation can be understood in terms of varying amounts of $^{56}$Ni produced and hence variation in the temperature of the ejecta.

## 3. The Observation of 42 SNe

In an ongoing systematic search we have, over the last 6 years, discovered and studied over 75 SNe. The majority of these were the most distant SNe ever observed. We have now completed the analysis of 42 of these SNe. The analysis of the first 7 of our SNe has already been published (Perlmutter, 1997)[2]. An additional SN at $z = 0.83$ has been measured with the Hubble Space Telescope and added to this sample, Perlmutter (1998a)[4]. The first analysis of a 40-supernova sample was presented at the January 1998 meeting of the American Astronomical Society (Perlmutter, 1998b)[5]; The current more extensive analysis[6] agrees with those results—as well as with a subsequent analysis of 16 SNe by the Hi-Z Supernova Search Team (Riess et al. 1998) [17].

When we bagan our program, only one high-redshift supernova had been discovered (18 days past maximum).[16] We developed a technique that made it possible to discover *batches* of high-redshift supernovae, while still on the rise to maximum light, in a systematic, predictable way. About twice a year, during two sets of 2 nights at the telescope, our procedure is to take about 50 - 70 different CCD images, depending on the depth in redshift we are trying to achieve. Each image covers about $15 \times 15$ square minutes of arc on the sky. The total area covered is thus about 3-4 square degrees. The first set of images are considered as "reference" images. The second set observed about 3 weeks later, are the "search" images in which we hunt for the new light due to a supernova. The timing relative to the moon is critical since we deal with such dim objects that they are difficult to observe at or near full moon. We take our reference images just after the new moon and our search images just before the next new moon. After discovery we take followup images of the SNe as well as spectra.

The new supernovae in this sample of 42 were all discovered while still brightening, using the Cerro Tololo 4-meter telescope with the $2048^2$ prime-focus CCD camera or the $4 \times 2048^2$ Big Throughput Camera. The supernovae were followed with photometry over the peak of their lightcurves, and approximately two - three months further ($\sim$40-60 days restframe) using the CTIO 4-m, WIYN 3.6-m, ESO 3.6-m, INT 2.5-m, and WHT 4.2-m telescopes. (SN 1994ap and other more recent supernovae have also been followed with HST photometry.) The supernova redshifts and spectral identifications were obtained using the Keck I and II 10-m telescopes with LRIS and the ESO 3.6-m telescope. We have observed spectra of the host galaxies for all of these. SNe spectra were observed for almost all SNe after the first 6 SNe. The pho-

tometry coverage was most complete in Kron-Cousins $R$-band, with Kron-Cousins $I$-band photometry coverage ranging from two or three points near peak to relatively complete coverage paralleling the $R$-band observations.

## 4. The Light Curve and $K$-corrections

We compare our measurements to nearby SN light curves measured with a blue filter. Because of the large redshift, the spectral features captured in the blue filter appear in the "red." We thus carry out our measurements with a red filter and then translate our measurements into the blue. As it turned out, this correction—called a $K$-correction—was particularly straightforward for our first distant SN because $1 + z = 1.458$ gives the ratio of the redshifted wavelength to the wavelength at emission. This value turned out to be the ratio of the central wavelength transmitted by our red filter to that of the blue filter, used for the nearby standard light curve. The acceptance width of the two filters were also roughly in this same ratio. For other z values the $K$-correction is a function of the epoch on the light curve and the stretch. The procedure modifies the light curve to allow for changes in the portion of the spectrum captured by each filter, Kim et al.[7] and Nugent et al.[8] .

## 5. Our Method for Obtaining $\Omega_M$ and $\Omega_\Lambda$

Our method for obtaining both $\Omega_M$ and $\Omega_\Lambda$ is discussed in Perlmutter et al.[2,6] and Goobar and Perlmutter[9].

To obtain $\Omega_M$ and $\Omega_\Lambda$ we make use of the following measurements:

- The redshift of the supernova or parent galaxy, $z$ is related to the wavelength change $\lambda - \lambda_o$ of the receding object. Here $z$ is defined as $z = (\lambda - \lambda_o)/\lambda_o$ and $\lambda_o$ is the wavelength in the rest system while $\lambda$ is the measured wavelength for identified lines. This requires taking a spectrum of the SN, to identify type Ia SN, whenever possible as well as of the galaxy for an accurate redshift determination.

- The apparent magnitude $m_B$ of the high-redshift SN at the peak of its light curve, calibrated to a standard lightcurve width ($s$=1). This is based on measurement of the SN light intensity as a function of time (generally in two filters), the photometry calibration, $K$-corrections, and a fit to the lightcurve to obtain the peak brightness and the lightcurve width $s$. (The two-filter measurements make it possible to characterize the extinction due to dust that reddens the light.)

- The same measurements obtained for a group of 18 well measured nearby Type Ia SNe from the Calán/Tololo Supernova Survey [10–12] .

The relation between the measured apparent magnitude $m_R$ and the absolute magnitude $M_B$ for type Ia SN, is given by

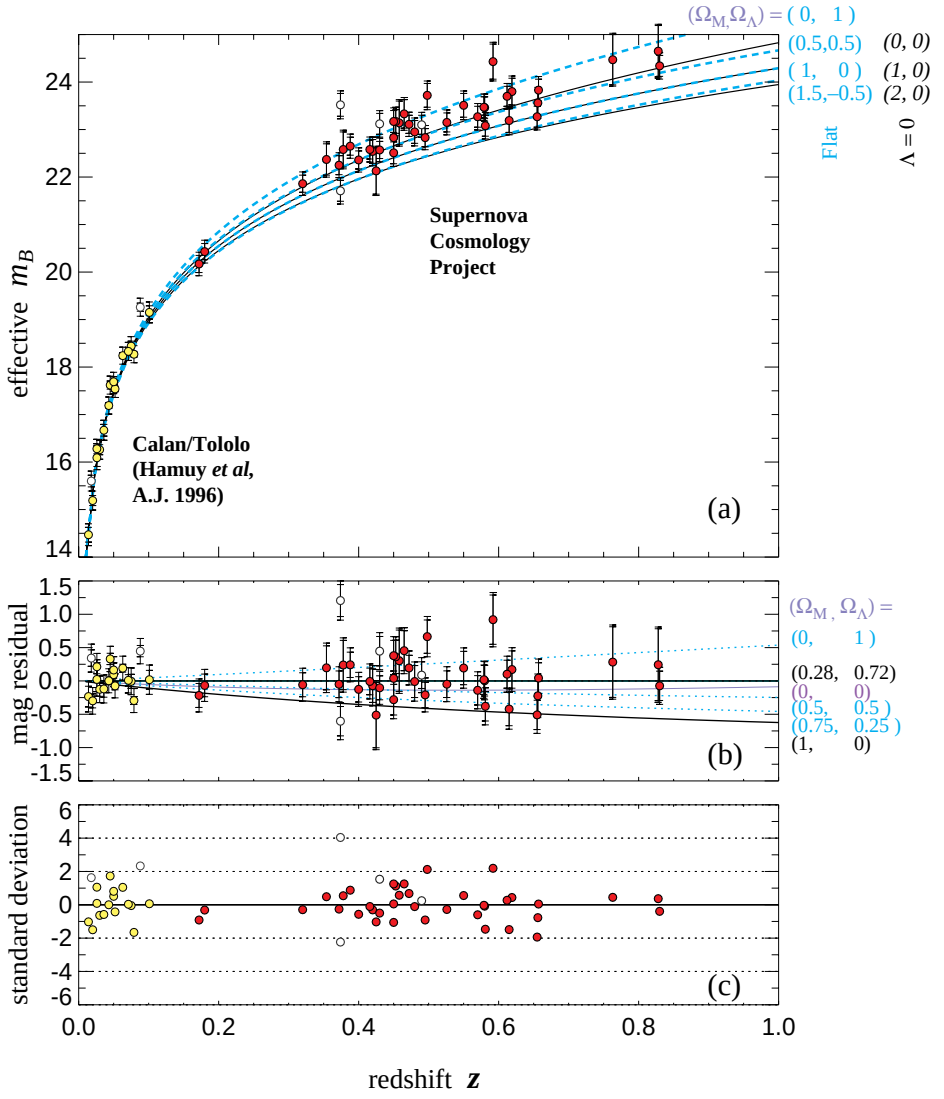


Figure 1: (a) Hubble diagram for 42 high-redshift SNe Ia from the Supernova Cosmology Project, and 18 low-redshift SNe Ia from the Calán/Tololo Supernova Survey, after correcting both sets for the SN Ia lightcurve width-luminosity relation. The inner error bars show the uncertainty due to measurement errors, while the outer error bars show the total uncertainty when the intrinsic luminosity dispersion, 0.17 mag, of lightcurve-width-corrected SNe Ia is added in quadrature. The unfilled circles indicate supernovae not included in Fit C. The solid curves are the theoretical $m_B^{\rm effective}(z)$ for a range of cosmological models with zero cosmological constant as indicated on the figure. (b) The magnitude residuals from the best-fit flat cosmology for the Fit C supernova subset, $(\Omega_{\rm M}, \Omega_\Lambda) = (0.28, 0.72)$. The curves are for a range of flat cosmological models as indicated on the figure. (c) The uncertainty-normalized residuals from the best-fit flat cosmology for the Fit C supernova subset, $(\Omega_{\rm M}, \Omega_\Lambda) = (0.28, 0.72)$.

$$m_R = 5 \log D_L + M_B + 25 + K_{RB} \quad (1)$$

Here $K_{RB}$ is the $K$-correction factor between red and blue SNe magnitudes, and $D_L = D_L(z; \Omega_m, \Omega_\Lambda, H_o)$ is the luminosity distance given here in Mpc ($\approx$ 3 million light years). Here $H_o$ is the Hubble constant, $c$ the velocity of light, $z$ is the measured red shift, usually obtained from the spectrum of the host galaxy. At first sight it appears that $D_L$ depends on the Hubble constant $H_o$ as well. However it turns out that the Hubble constant cancels because $H_o$ also appears in the determination of $M_B$ obtained from type Ia SN measurements in nearby galaxies Hamuy et al[10–12].

Fig.1 shows $m_B^{\rm effective}$ for our 42 SNe as well as the 18 Calán/Tololo Supernova Survey SNe plotted against redshift. The curves represent the Hubble diagram for a variety of cosmological models as indicated on the figure. The fit to the expression for $D_L$ gives an approximately linear relation between $\Omega_M$ and $\Omega_\Lambda$ in the region of interest ($\Omega_M < 1.5$). Our best fit is illustrated in Fig. 2. We have carried out a series of fits under somewhat different data selections, e.g. (A) all the data, (B) with 2 outlying SNe removed, (C) with 2 reddened and 2 extreme stretch SNe removed, etc. (see Perlmutter et al. 1998c for details)[6]. Our results are quite stable with respect to these various sample selections. In particular, one fit was made with *no* stretch corrections, and this yielded a fit completely consistent with our results *with* stretch corrections. We have used the two-filter color measurements to study the possible effect of extinction due to dust that reddens the supernova light, and find that our results are robust with respect to this effect (again, see Perlmutter[6] for details).

Our measurements have to be carried out at cosmological distances i.e., large values of $z$ since for small $z$ values $z < 0.11$, the dependence on $\Omega$ is negligible and the luminosity distance becomes $D_L = {\rm cz/H}_o$.

## 6. Type Ia Supernovae as Clocks at Cosmological Distances

We will now make use of the "standard" nature of the SNe Ia light curve shapes. This feature allows us to consider the SNe Ia as "clocks" at cosmological distances. As discussed above SNe Ia are, as a class highly homogeneous, since they are thermonuclear explosions that are apparently triggered under very similar physical conditions.

The work of Phillips[1], Hamuy [10–12] and Riess, Press & Kirshner[19], have emphasized the *inhomogeneity* of Type Ia light curve shapes, particularly for the "non-normal" redder Type Ia's. Perlmutter [2,6] provided a single-parameter characterization of these light curve differences, which is simply a time-axis stretch factor, $s$, which stretches (or compresses) the Leibundgut template light curve. From this study based on *nearby* SNe it was shown that this stretch factor $s$ extends over a range of 0.80 to 1.20 with an occasional outlier outside these values. Light curve shapes have been found to be correlated with peak magnitudes, UV colors, spectral features, etc. [2] We will now show data obtained by treating 36 of these SNe with $0.30 < z < 0.70$ as a group.

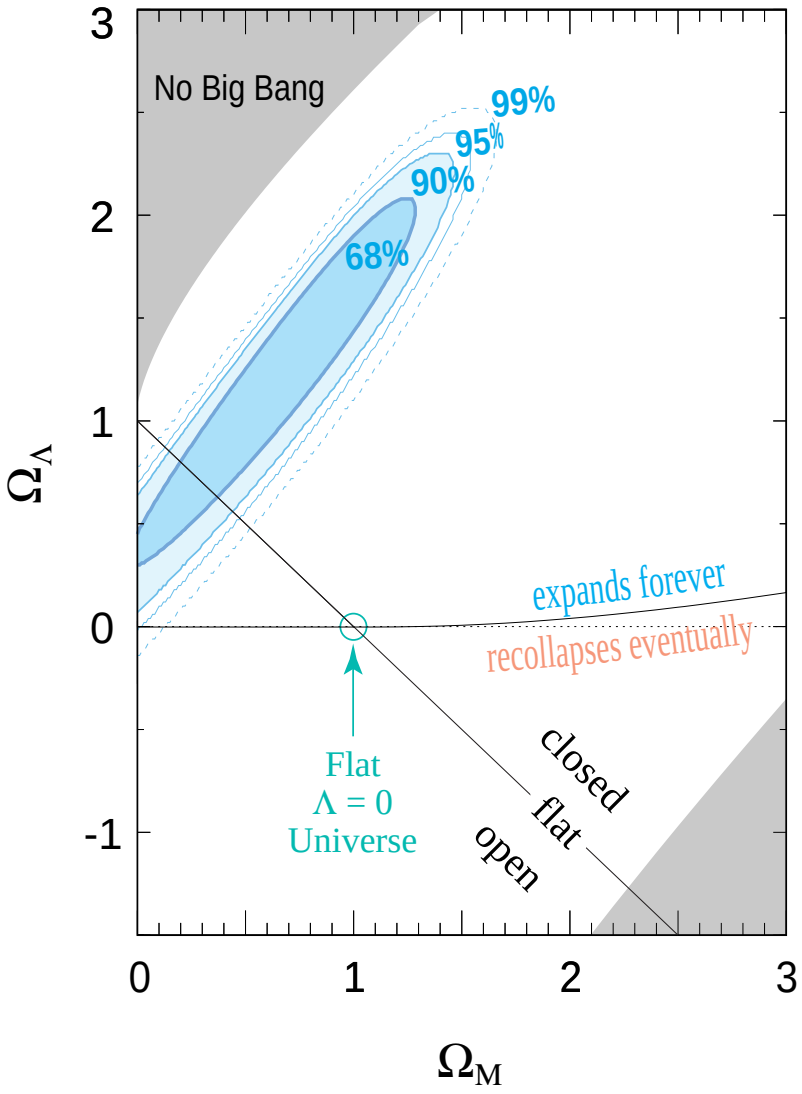


Figure 2: The 68%, 90%, 95%, and 99% confidence regions in the $\Omega_M$–$\Omega_\Lambda$ plane from Perlmutter et al.[6] (see this reference for details of the fit procedure). (The table of this two-dimensional probability distribution is available at http://www-supernova.lbl.gov/.) In cosmologies above the near-horizontal line the universe will expand forever, while below this line the expansion of the universe will eventually come to a halt and recollapse. This line is not quite horizontal because at very high mass density there is a region where the mass density can bring the expansion to a halt before the scale of the universe is big enough that the mass density is dilute with respect to the cosmological constant energy density. The upper-left shaded region, labeled "no big bang," represents "bouncing universe" cosmologies with no big bang in the past.The lower right shaded region corresponds to a universe that is younger than the oldest heavy elements, for any value of $H_0 \geq 50$ km s$^{-1}$ Mpc$^{-1}$.

Using supernova light curves to test the cosmological expansion was first suggested by Wilson[18] 1939. Over the last decade it has become clear what superb and precise clocks located both nearby and at cosmological distances SNe Ia are.

We presented the first clear observation of this time-dilation effect based on our first seven high z type Ia SNe at the 1995 conference at Aigua Blava, Spain, Goldhaber[13]. Later Leibundgut et al.[14] gave confirmatory evidence for time-dilation, based a single high z supernova. More recently, Riess et al. [20] 1997 showed evidence that the spectral features of SNe Ia can be timed sufficiently well to measure the time interval between two spectra taken 10 days appart in the observer system. Applying this method to 1 SN gave results consistent with the time-dilation factor $1+z$ at the 96.4% confidence level.

## 7. Fit to the Light Curve.

In our data analysis we fit each of our observed SNe lightcurve points to $R$-band template light curves using the fitting program MINUIT (James and Roos 1994). Each $R$-band template is constructed from the $B$-band rest system Leibundgut template and the appropriate cross filter $K$-correction[7,8].

Each SN is fit for three variables: the day and magnitude of peak light and the width factor $w = s(1+z)$ by which the Leibundgut curve had to be expanded. In the present analysis we make use of the day at peak to align all the 36 SNe light curves, we normalize the flux of each SN to unity. As these SNe are measured in the $R$-band we now translate the points to the $B$-band. The individual photometry points are $K$-corrected [7,8] from the measured $R$-band photometry points to the $B$-band where lower z data is available for comparison[10–12]. Two SNe at z=0.18 and 3 at $z > 0.7$ have to be $K$-corrected to the $V$-band and $U$-band respectively and are thus not included here. One distinct outlier, SN97O is also left out here.

## 8. Analysis of 36 Supernavae treated as a Group.

The stretch factor affects our ability to test time dilation, since the expected dilation factor $1+z$ is modified by the stretch factor $s$. The observable effect is then $w = s(1+z)$. Fig.3a shows the distribution of $w$ for SCP data (solid histogram) and Calán/Tololo data (dashed histogram). Fig.3b shows the corresponding histograms for $s$.

If no independent $s$ corrections are made to our width measurements, an additional dispersion of $x$ is observed, assuming a similar population of SNe at high redshift.

Fig. 4a shows the distribution of $w$ vs. $1+z$ for both the Calán/Tololo data and the SCP data. As can be noted , except for 2 outliers in the SCP data and 3 in the Calán/Tololo data, $0.8 < s < 1.2$. In Fig. 4b we show the stretch distribution $s$ vs. $1+z$.

In Fig.5a we show the $R$-band photometry points, individualy $K$-corrected to the $B$-band for the SNe with $0.30 < z < 0.70$, aligned at maximum light in the observer

system. The measured points for SNe with $0.45 \leq z < 0.70$ are shown in red, the points from SNe with $0.30 < z < 0.45$ are shown in green. Also shown are are points (violet) from the 18 SNe from the Calán/Tololo study in the $B$-band (Hamuy 1996) with $z < 0.11$, these are also $K$-corrected. These 18 SNe were chosen out of 29 SNe by having been discovered prior to 5 days after maximum light. Fig 3b shows the same data averaged over all SNe in each z band. Fig.5b shows the same data with the SCP data averaged over the entire $0.30 < z < 0.70$ interval and averaged over 2 days. Finally we also show the rest system Leibundgut curve extended down to the explosion time Nugent et al.[23] 1999, Goldhaber, Groom et al.[24] 1999 . These figures illustrate the time dilation effect clearly. The width of the light curves are $z$ dependent in the observer system. The nearby SNe (violet points) approximate the rest system curve while the high redshift data (green and red points) give wider distributions. This time dilation is particularly clear in Fig.5c. The (violet) low-z points follow the curve while the (green) outer points are clearly much wider, indicating time-dilation.

If we now transform the time axis from the observer frame to the rest frame by dividing by the appropriate 1+z for each data point of each of the SNe and then divide the time axis by $s$ as well, Fig. 6a and 6b we note excellent overlap of all the individual photometry points. Thus with one parameter $s$ and the time dilation $1+z$ all the normalized and aligned SNe fit a single curve. The relations between stretch, color and brightness as noted by Riess et al[19] will be discussed in detail in terms of stretch in an upcoming publication Kim, Aldering et al.1999[22] .

## 9. Time Dilation and Doppler Shift - an Example

The time dilation effect can be understood in terms of the Doppler shift. We present a simple example of this.

We note that the upper limit of the observed redshift $z = 0.7$ corresponds to $\beta = 0.49$ and that $\beta = 0.5$ corresponds to $z = 0.73$. Consider 2 points in time on the light curve symmetric around the peak and 4 weeks appart, in the SN rest system for $z = 0.73$. When the light emitted from the first point reaches us we start our clock in the observer frame. When the light is emitted from the second point the SN will, by the expansion of the universe, be at a greater distance from our telescope. With $\beta = 0.5$, this extra distance will be 2 light weeks. From this clasical effect alone the two points in the observer system will be 6 weeks appart, a time dilation of 1.5. Thus the time-dilation measures the expansion of the Universe directly. The relativistic version is given by $1+z = \sqrt{((1+\beta)/(1-\beta))}$ which equals $\gamma(1+\beta)$ where $\gamma = 1/\sqrt{(1-\beta^2)}$. For the redshift values we are dealing with the $\gamma$ factor is only a small correction 1.15 to give 6.93 weeks in the observer frame. The main effect we are observing is thus the direct expansion of the universe. The same argument also holds for the redshift of the light emmitted by the SN where we now think of the 2 points as two adjacent crests of the light wave.

## 10. References

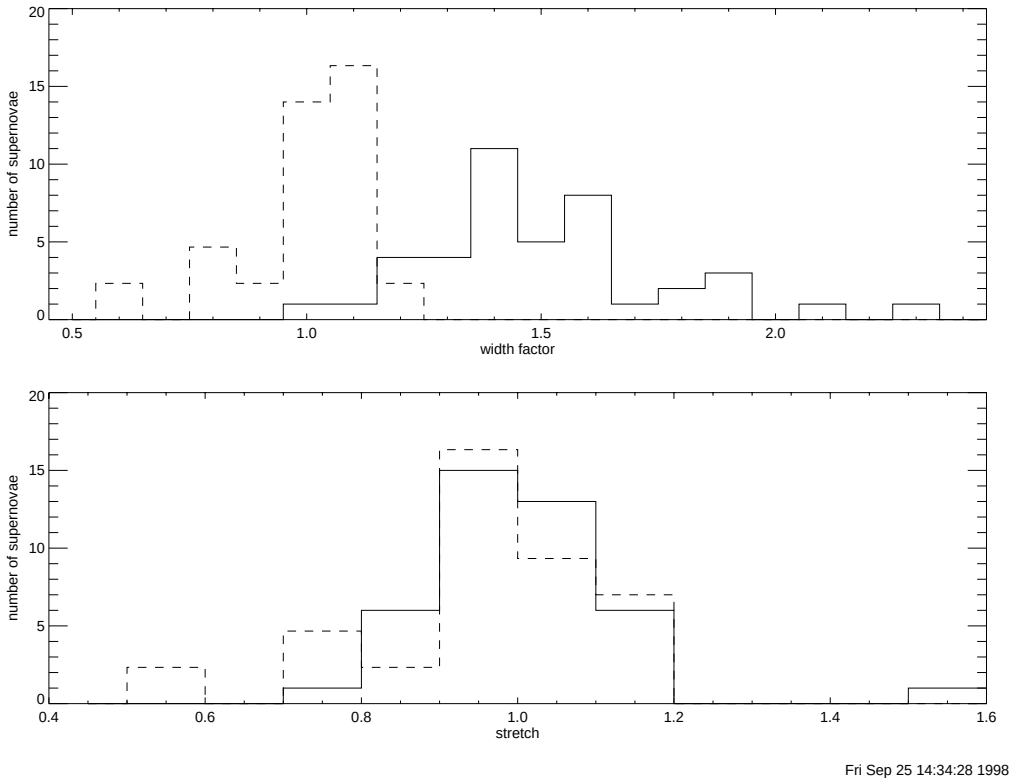


Figure 3: a. The distribution of the observed lightcurve width $w$ for the 18 of the Calán/Tololo SNe (brocken line histogram) with area normalized to 42 and the SCP data for 42 fully analysed SNe (solid line histogram). b. The corresponding stretch distributions $s$ defined as the observed lightcurve width divided by $1+z$ for each SN.

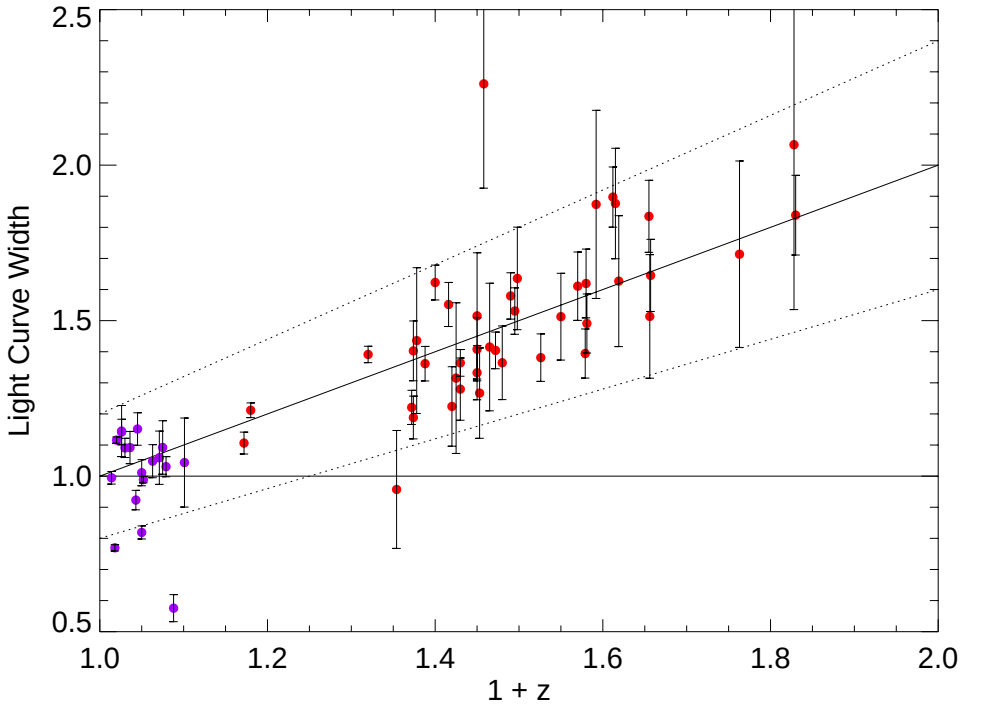


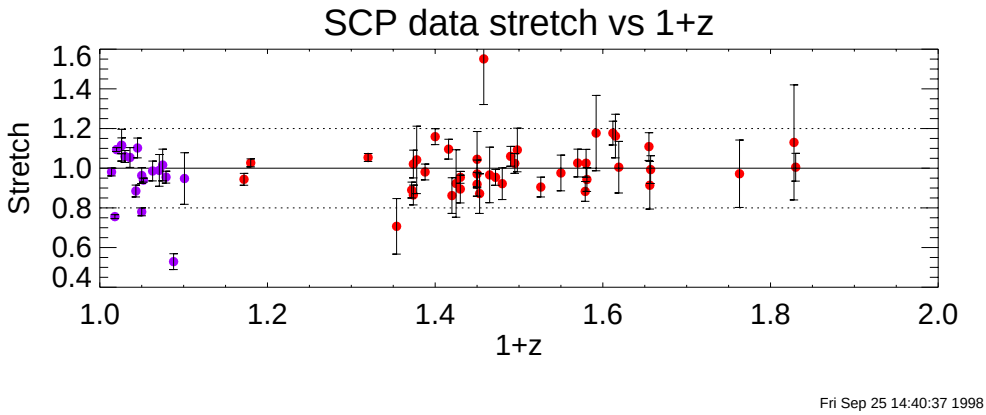


Figure 4: *a*. The Observed Lightcurve Width vs $1+z$. The (violet) points for $z < 0.11$ are the Calán/Tololo SNe, the (red) points for $z > 0.5$ are the SCP data for 42 fully analysed SNe. The band delineated by the dotted lines corresponds to stretch values 0.8 to 1.2 which encompass the bulk of the data, except for a few outliers. *b*. The stretch $s$ vs $1+z$. Stretch is defined as the Observed Lightcurve Width $w$ divided by $1+z$ for each SN.The points and lines are defined as in *a*.

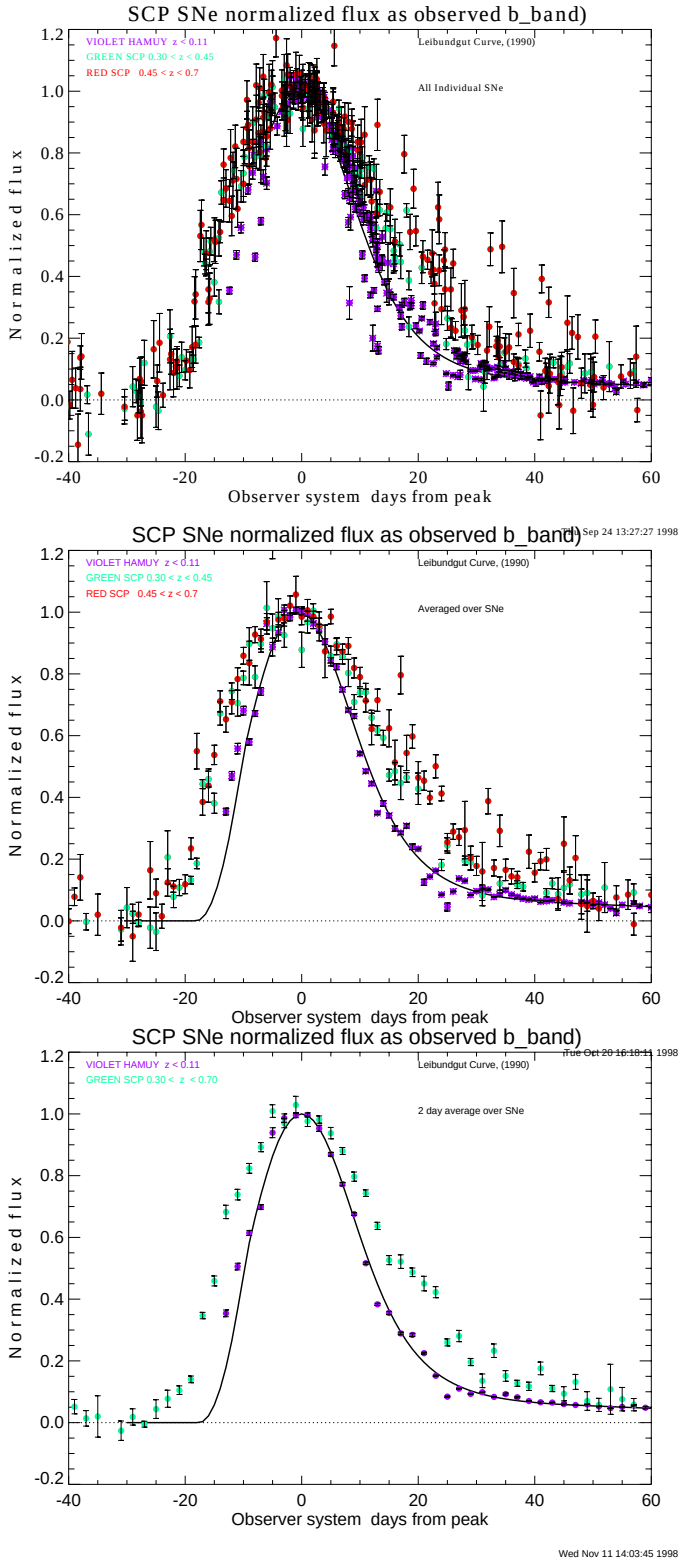


Figure 5: *a*. The photometry points for the 34 SCP and 18 Calán/Tololo SNe, flux normalized to unity and aligned at the peak in the observer system. *b* The same data as in *a* averaged over each day. The Leibundgut light-curve extended to explosion time[23,24] is also shown, to indicate the rest system. *c* The SCP data for $0.30 < z < 0.70$ and the Calán/Tololo SNe averaged over 2 days, compared with the extended Leibundgut light-curve.

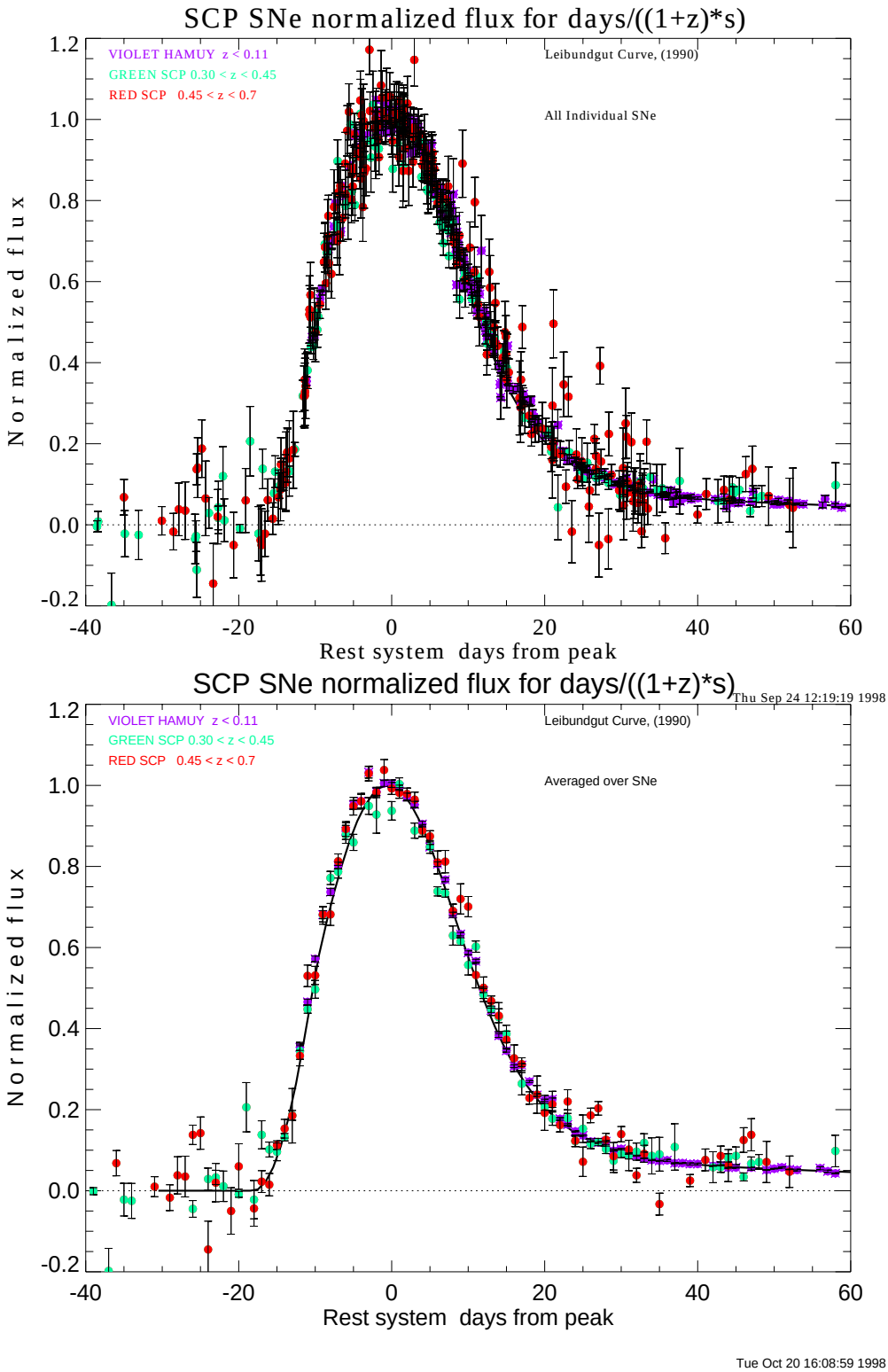


Figure 6: *a* The photometry points for the same 3 sets of SNe, transformed to the rest system and corrected for the stretch factor $s$. *b* The same data as in *a* averaged over each day. All the points are consistent with the extended Leibundgut curve[24] indicating that the single parameter $s$ combined with the expansion factor $1+z$ fall on a unique curve.

1. Phillips, M. M. 1993. Ap.J., 413, L105.
2. Perlmutter, S., et al. 1997. Ap.J., 483,565 .
3. Leibundgut, B. 1991. Supernovae, ed. S.E. Woosley, (New York: Springer), 751.
4. Perlmutter, S., et al. 1998a. Nature, 391, 51 and erratum (on author list), 392, 311
5. Perlmutter, S., et al. 1998b. Ap.J., LBL-42230: "Presentation at the January 1998 Meeting of the American Astronomical Society," available at www-supernova.LBL.gov and astro-ph; referenced in B.A.A.S., vol. 29, p. 1351 (1997).
6. Perlmutter, S., et al. 1998c. Ap.J., submitted. Also available at www-supernova.LBL.gov and astro-ph.
7. Kim, A., Goobar A., & Perlmutter S. 1996. P.A.S.P., 108:190.
8. Nugent, P. et al. 1999. P.A.S.P., in preparation .
9. Goobar A., & Perlmutter S. 1995. Ap.J., 450,14 .
10. Hamuy, M., Phillips, M. M., Wells, L. A., & Maza, J. 1993. PASP, 105:787
11. Hamuy, M., et al. 1993b. A.J. 106:2392
12. Hamuy, M., Phillips, M. M., Maza, J., Suntzeff, N.B., Schommer, R., & Aviles, R. 1995. Ap.J., 109:1
13. Goldhaber, G., et al. 1995. In Presentations at the NATO ASI in Aiguablava, Spain, LBL-38400, page III.1; also published in Thermonuclear Supernova, P. Ruiz-Lapuente, R. Canal, and J.Isern, editors, Dordrecht: Kluwer, page 777 (1997)
14. Leibundgut, B., et al. 1996. Ap.J. Lett., 466,L21 .
15. D. Branch and G.A. Tammann 1992. Ann. Rev. Astron. Astrophys., 30, 359–89.
16. Norgaard-Nielsen, et al. 1989. Nature, 339, 523
17. Riess, A. G., et al. 1998, ApJ, 116, 1009
18. Wilson, O. C. 1939, A.J. 90, 634
19. Riess, A. G., Press, W. H., & Kirshner, R. P. 1995, ApJ, 438, L17 & 1996, ApJ, 473, 88
20. Riess, A. G. et al. 1997. A.J., 114(2), 722
21. Kim, A., Aldering, G. et al. 1999. ApJ, in preparation
22. Nugent, P. et al. 1999. ApJ, in preparation
23. Goldhaber, G., Groom, D., et al. 1999. ApJ, in preparation